Impairment of a distinct cancer-associated fibroblast population limits tumour growth and metastasis

Ute Jungwirth, Antoinette van Weverwijk, Liam Jenkins, John Alexander, David Vicente, Qiong Gao, Syed Haider, Marjan Iravani and Clare M. Isacke

SUPPLEMENTARY MATERIAL

Supplementary methods

Supplementary Tables 1 - 4

Supplementary Table 1a. | Top 30 upregulated pathways in D2A1-m12 cells compared to D2A1 cells

Supplementary Table 1b. | Top 30 downregulated pathways in D2A1-m12 cells compared to D2A1 cells

Supplementary Table 2 | Antibodies

Supplementary Table 3 | Mission shRNA lentiviral particles targeting Endo180 (*Mrc2*) (Sigma)

Supplementary Table 4 | ON-TARGET *plus* siRNA targeting Endo180 (*Mrc2*) (Dharmacon)

Supplementary Figures 1 - 7

Supplementary Fig. 1 | Fibroblast expression of Endo180 in solid tumours

Supplementary Fig. 2 | Endo180 promotes metastatic tumour growth in lungs and liver

Supplementary Fig. 3 | Expression of Endo180 in the brain

Supplementary Fig. 4 | Endo180 expression following siRNA- or shRNA-mediated knockdown

Supplementary Fig. 5 | Fibroblast-tumour cell co-culture assays

Supplementary Fig. 6 | Cell spreading on collagen or fibronectin-coated hydrogels

Supplementary Fig. 7 | Comparison of the parental D2A1 line and the D2A1-m12 subline

Supplementary methods

Whole exome sequencing

DNA was extracted from tumour cell lines or BALB/c mouse spleen tissue using the DNeasy Blood and Tissue kit. DNA samples were physically sheared to the desired size using a Covaris E Series instrument (Covaris). Paired-end multiplexed library preparation was performed by the Tumour Profiling Unit at the ICR using the SureSelect^{XT} Library Prep and Capture System (Agilent Technologies) following the standard protocol workflow, before multiplex sequencing on a NovaSeq 6000 flow cell (Illumina).

Bioinformatics and statistical analyses were performed using custom R scripts and a bespoke DNA sequencing pipeline based on the Nextflow framework[1]. Whole exome sequencing FASTQ files were aligned to the mouse genome assembly build GRCm38 with the Burrows-Wheeler Aligner (BWA) v0.7.12[2]. BWA was run with default parameters utilising 5 threads. The resulting SAM file was converted to BAM and sorted with SAMtools v1.5[3]. Duplicate reads were removed from the sample files with the Picard v2.8.1 suite of tools (http://broadinstitute.github.io/picard/). Insert size and coverage metrics were also calculated with Picard. Lastly, base scores were recalibrated with the Genome Analysis Toolkit (GATK) v4.0.3.0[4] according to the GATK Best Practices pipeline.

Copy number analysis (CNA) was carried out with CNVkit v0.9.3[5], utilising the batch command. A cancer-free sample taken from BALB/c mouse spleen tissue was used as a normal reference for each cell line sample. Copy number $\log_2$ ratios from CNVkit were used to create CNA plots in R statistical programming language v3.5.0 (R Core Team, 2018).

LoFreq[6] was used to call somatic variants. In CNA, the same healthy BALB/c sample was used as a normal reference. Common variants were removed before annotating the remaining variants with ANNOVAR (01/02/2016 release)[7]. The output from ANNOVAR was further processed in R for comparisons between samples and visualisations.

Supplementary Tables

Supplementary Table 1a. | Top 30 upregulated pathways in D2A1-m12 cells compared to D2A1 cells		
Pathway	NES	FDR
mouse.corematrisome.collagens	1.886	0.038
mouse.matrisome.associated.ecm.affiliated	1.869	0.019
mouse.corematrisome.glycoproteins	1.836	0.024
BIOCARTA_MM_CASPASE_CASCADE_IN_APOPTOSIS	1.793	0.058
BIOCARTA_MM_THROMBIN_SIGNALING_AND_PROTEASE-ACTIVATED_RECEPTORS	1.792	0.038
BIOCARTA_MM_D4-GDI_SIGNALING_PATHWAY	1.732	0.038
PANTHER_MM_INTEGRIN_SIGNALLING_PATHWAY	1.729	0.019
BIOCARTA_MM_RHO_CELL_MOTILITY_SIGNALING_PATHWAY	1.633	0.224
mouse.matrisome.associated.regulators	1.582	0.079
PANTHER_MM_HETEROTRIMERIC_G-PROTEIN_SIGNALING_PATHWAY-GI_ALPHA_AND_GS_ALPHA_MEDIATED	1.562	0.179
PANTHER_MM_FAS_SIGNALING_PATHWAY	1.548	0.345
BIOCARTA_MM_PHOSPHOLIPIDS_AS_SIGNALLING_INTERMEDIARIES	1.540	0.353
BIOCARTA_MM_RAC_1_CELL_MOTILITY_SIGNALING_PATHWAY	1.533	0.371
BIOCARTA_MM_INTEGRIN_SIGNALING_PATHWAY	1.525	0.345
BIOCARTA_MM_RAS-INDEPENDENT_PATHWAY_IN_NK_CELL-MEDIATED_CYTOTOXICITY	1.522	0.371
PANTHER_MM_IONOTROPIC_GLUTAMATE_RECEPTOR_PATHWAY	1.511	0.371
BIOCARTA_MM_ROLES_OF_ARRESTIN-DEPENDENT_RECRUITMENT_OF_SRC_KINASES_IN_GPCR_SIGNALING	1.493	0.393
PANTHER_MM_INFLAMMATION_MEDIATED_BY_CHEMOKINE_AND_CYTOKINE_SIGNALING	1.489	0.156
BIOCARTA_MM_ROLE_OF_ARRESTINS_IN_THE_ACTIVATION_AND_TARGETING_OF_MAP_KINASES	1.477	0.399
BIOCARTA_MM_SPLICEOSOMAL_ASSEMBLY	1.470	0.399
BIOCARTA_MM_CCR3_SIGNALING_IN_EOSINOPHILS	1.467	0.403
BIOCARTA_MM_TGF_BETA_SIGNALING_PATHWAY	1.464	0.399
NETPATH_MM_ALPHA6_BETA4_INTEGRIN	1.423	0.371
NETPATH_MM_EGFR1_SIGNALING_PATHWAY	1.415	0.038
mouse.matrisome.associated.secretedfactors	1.409	0.345
PANTHER_MM_CYTOSKELETAL_REGULATION_BY_RHO_GTPASE	1.408	0.393
NETPATH_MM_B_CELL_RECEPTOR_SIGNALING_PATHWAY	1.403	0.314
PANTHER_MM_HETEROTRIMERIC_G-PROTEIN_SIGNALING_PATHWAY-GQ_ALPHA_AND_GO_ALPHA_MEDIATED	1.382	0.421
PANTHER_MM_HUNTINGTON_DISEASE	1.377	0.371
BIOCARTA_MM_MTOR_SIGNALING_PATHWAY	1.357	0.602
BIOCARTA_MM_TREFOIL_FACTORS_INITIATE_MUCOSAL_HEALING	1.352	0.602
Pathways highlighted in yellow have FDR < 0.1. FDR, false discovery rate. NES, normalised enrichment score		

Supplementary Table 1b. | Top 30 downregulated pathways in D2A1-m12 cells compared to D2A1 cells		
Pathway	NES	FDR
BIOCARTA_MM_SYNAPTIC_PROTEINS_AT_THE_SYNAPTIC_JUNCTION	-1.606	0.345
PANTHER_MM_SYNAPTIC_VESICLE_TRAFFICKING	-1.531	0.391
PANTHER_MM_INSULIN_IGF_PATHWAY-PROTEIN_KINASE_B_SIGNALING_CASCADE	-1.527	0.371
PANTHER_MM_METABOTROPIC_GLUTAMATE_RECEPTOR_GROUP_I_PATHWAY	-1.429	0.558
BIOCARTA_MM_BONE_REMODELLING	-1.404	0.602
BIOCARTA_MM_REGULATION_OF_EIF2	-1.400	0.600
PANTHER_MM_EGF_RECEPTOR_SIGNALING_PATHWAY	-1.321	0.393
BIOCARTA_MM_TELOMERES_TELOMERASE_CELLULAR_AGING_AND_IMMORTALITY	-1.299	0.646
PANTHER_MM_MUSCARINIC_ACETYLCHOLINE_RECEPTOR_1_AND_3_SIGNALING_PATHWAY	-1.272	0.614
BIOCARTA_MM_TOLL-LIKE_RECEPTOR_PATHWAY	-1.271	0.602
PANTHER_MM_P53_PATHWAY_FEEDBACK_LOOPS_2	-1.269	0.602
PANTHER_MM_CORTOCOTROPIN_RELEASING_FACTOR_RECEPTOR_SIGNALING_PATHWAY	-1.264	0.667
PANTHER_MM_PI3_KINASE_PATHWAY	-1.259	0.602
BIOCARTA_MM_CD40L_SIGNALING_PATHWAY	-1.248	0.704
PANTHER_MM_PDGF_SIGNALING_PATHWAY	-1.222	0.568
PANTHER_MM_HISTAMINE_H1_RECEPTOR_MEDIATED_SIGNALING_PATHWAY	-1.205	0.692
PANTHER_MM_INTERLEUKIN_SIGNALING_PATHWAY	-1.188	0.656
BIOCARTA_MM_INHIBITION_OF_CELLULAR_PROLIFERATION_BY_GLEEVEC	-1.186	0.757
PANTHER_MM_INSULIN_IGF_PATHWAY-MITOGEN_ACTIVATED_PROTEIN_KINASE_KINASE_MAP_KINASE_CASCADE	-1.177	0.753
BIOCARTA_MM_P53_SIGNALING_PATHWAY	-1.094	0.808
PANTHER_MM_OXIDATIVE_STRESS_RESPONSE	-1.092	0.795
BIOCARTA_MM_P38_MAPK_SIGNALING_PATHWAY_	-1.087	0.795
BIOCARTA_MM_KERATINOCYTE_DIFFERENTIATION	-1.087	0.795
BIOCARTA_MM_SKELETAL_MUSCLE_HYPERTROPHY_IS_REGULATED_VIA_AKT_MTOR_PATHWAY	-1.083	0.808
PANTHER_MM_HYPOXIA_RESPONSE_VIA_HIF_ACTIVATION	-1.067	0.808
BIOCARTA_MM_THE_4-1BB-DEPENDENT_IMMUNE_RESPONSE	-1.052	0.827
PANTHER_MM_OXYTOCIN_RECEPTOR_MEDIATED_SIGNALING_PATHWAY	-1.050	0.824
PANTHER_MM_5HT2_TYPE_RECEPTOR_MEDIATED_SIGNALING_PATHWAY	-1.031	0.827
PANTHER_MM_HISTAMINE_H2_RECEPTOR_MEDIATED_SIGNALING_PATHWAY	-1.023	0.872
BIOCARTA_MM_NEUROPEPTIDES_VIP_AND_PACAP_INHIBIT_THE_APOPTOSIS_OF_ACTIVATED_T_CELLS	-0.987	0.922
BIOCARTA_MM_CERAMIDE_SIGNALING_PATHWAY	-0.970	0.922
FDR, false discovery rate. NES, normalised enrichment score		

Supplementary Table 2 | Antibodies

Antibody	Species	Source (catalogue number)	Assays	Dilution
αSMA	mouse	Sigma (clone 1A4)	IHC	1:1,000
CD24	rat	eBioscience (M1/69)	FACS	4 µL/1x10^7cells/mL
CD45	rat	R&D Systems (MAB114)	FACS	4 µL/1x10^7cells/mL
Endo180 (human)	mouse	mAb 39.10 (in house)[8]	IHC	1:1,000
Endo180 (mouse)	sheep	R&D Systems (AF4789)	WB	1 µg/mL
Fibronectin	rabbit	Dako (A0245)	IF	1:2,000
MLC	rabbit	Cell Signaling (3672)	WB	1:1,000
p(ser19)-MLC	mouse	Cell Signaling (3675)	WB	1:1,000
Alexa488-phalloidin	N/A	Molecular Probes (A12379)	IF	1:500
Alexa555-phalloidin	N/A	Molecular Probes (A34055)	IF	1:500
DAPI	N/A	Molecular Probes (D1306)	IF	1:10,000
IgG-HRP-anti-mouse	donkey	Santa Cruz (sc-2314)	WB	1:10,000
IgG-HRP-anti-rabbit	goat	Santa Cruz (sc-2004)	WB	1:10,000
IgG-HRP-anti-sheep	rabbit	Santa Cruz (sc-2770)	WB	1:10,000

FACS, fluorescence activated cell sorting; IF, immunofluorescence; IHC, immunohistochemistry; WB, western blot.

Supplementary Table 3 | Mission shRNA lentiviral particles targeting Endo180 (*Mrc2*) (Sigma)

Clone ID	Gene target	NM ID
SHC002V	NTC	N/A
TRCN00001239-25	*Mrc2*	NM_008626.3
TRCN00001239-27	*Mrc2*	NM_008626.3
TRCN00001239-28	*Mrc2*	NM_008626.3

Supplementary Table 4 | ON-TARGET *plus* siRNA targeting Endo180 (*Mrc2*) (Dharmacon)

ID	Gene target	NM ID
D-001810-01	NTC	N/A
D-001810-04	NTC	N/A
J-040940-09	*Mrc2*	NM_008626.3
J-040940-12	*Mrc2*	NM_008626.3

Supplementary Figure 1

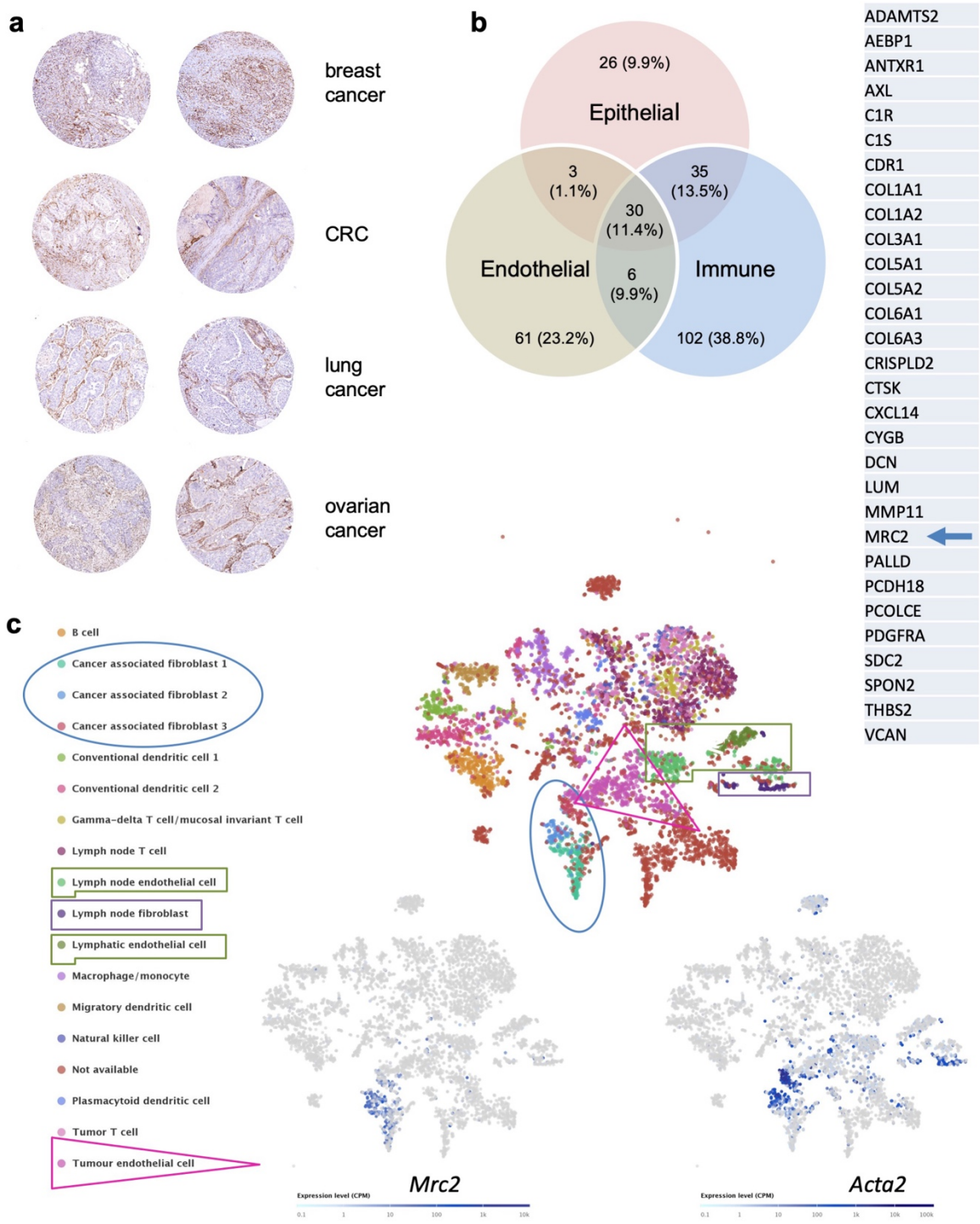

Supplementary Fig. 1 | Fibroblast expression of Endo180 in solid tumours

a Images taken from The Human Protein Atlas (www.proteinatlas.org) of breast, colorectal lung and ovarian tumours stained for Endo180. Related to Fig.1a, where a comparable pattern of Endo180 staining in human breast cancers is observed using an independent antibody. **b** Left panel, upregulated expression of genes with *P* value < 10^{-11} in CAFs compared to endothelial, immune or epithelial/tumour cell populations from the human colorectal cancer GSE39397 dataset[9]. Right panel, list of the 30 genes commonly upregulated in CAF *vs.* endothelial, CAF *vs.* immune and CAF *vs.* epithelial/tumour cells, with Endo180 (*MRC2*) highlighted. Related to Fig. 1b. **c** tSNE visualisation of stromal cells and colour coded cell types isolated from primary B16-F10 mouse melanoma tumours and draining lymph nodes and subject to single cell RNA-seq (bioRxiv doi.org/10.1101/467225). Expression of marker genes for each cell type, *Mrc2* (bottom left) and *Acta2* (bottom right) analysed from deposited data (https://www.ebi.ac.uk/gxa/sc/experiments/E-EHCA-2/Results). **d** Correlation of Endo180 (*MRC2)* gene expression with a fibroblast TGFβ response signature (F-TBRS)[9] in the luminal A, luminal B, HER2-enriched and basal-like breast cancer intrinsic subtypes in the TCGA dataset. Related to Fig. 1g.

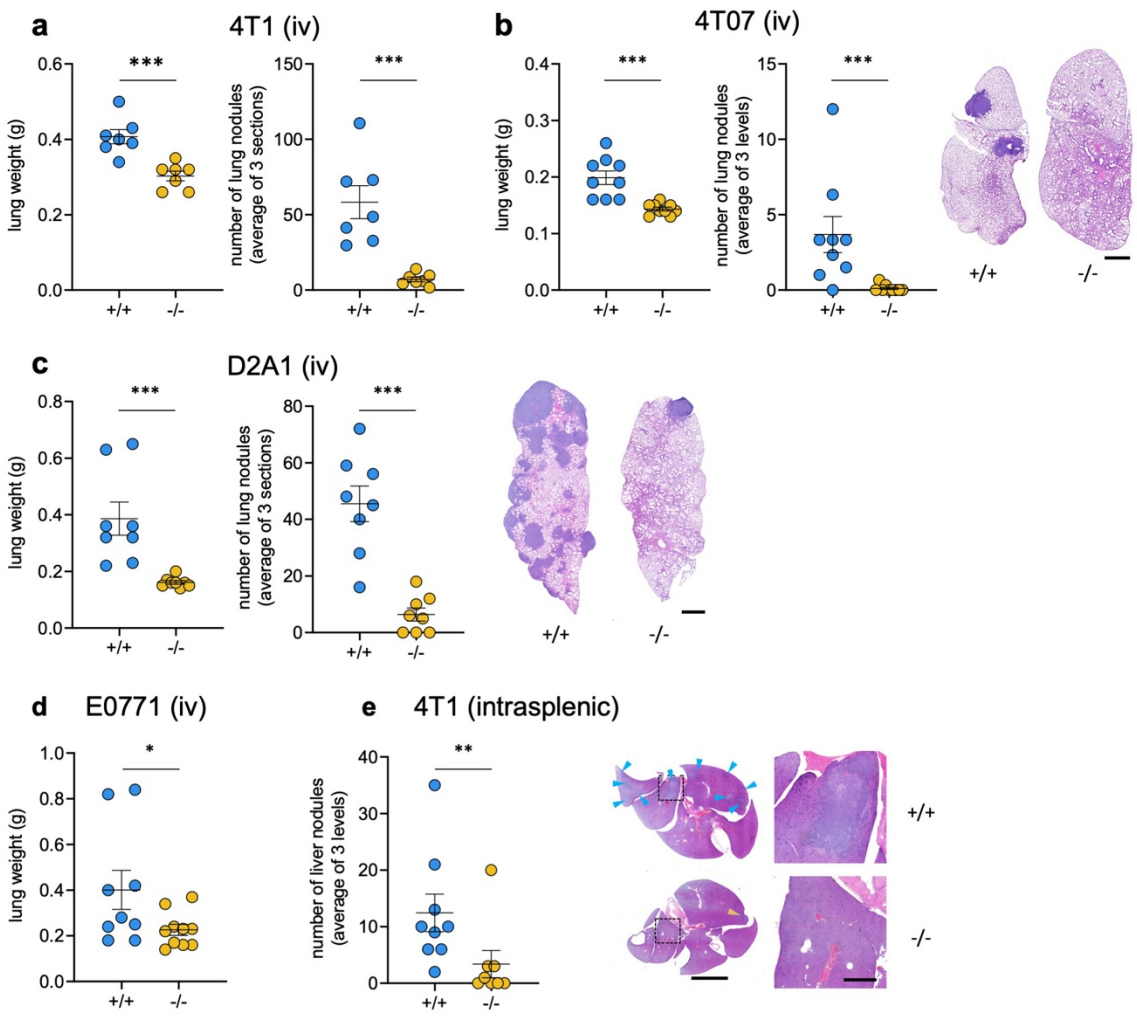

Supplementary Fig. 2 | Endo180 promotes metastatic tumour growth in lungs and liver

Additional quantification of the data presented in Figure 3. All data are mean values ±SEM. Quantification of metastatic nodules represents mean number of lung nodules in 3 lung or liver sections. **a** 4T1-Luc cells injected intravenously into BALB/c mice (n = 7 per group) from Figure 3a. Shown are *ex vivo* lung weights (*t*-test) and number of metastatic lung nodules (*t*-test). **b** 4T07 cells injected intravenously into BALB/c mice (n = 9 per group) from Figure 3b. Shown are *ex vivo* lung weights (*t*-test) and number of metastatic lung nodules (Mann-Whitney *U* test, scale bar, 1 mm). **c** D2A1 cells injected intravenously into BALB/c mice (n = 8 per group) from Figure 3c. Shown are *ex vivo* lung weights (Mann-Whitney *U* test), number of metastatic lung nodules (*t*-test) and representative H&E stained sections (scale bar, 1 mm). **d** E0771-Luc cells injected intravenously into C57BL/6 mice (n = 9 or 10 per group) from Figure 3e. Shown are *ex vivo* lung weights (Mann-Whitney *U* test). **e** 4T1-Luc cells injected into the spleen parenchyma of BALB/c mice (n = 8 or 9 per group) from Figure 3f. Shown are number of metastatic liver nodules (Mann-Whitney *U* test) and low (scale bar, 5 mm) and high power (scale bar, 1 mm) images of H&E stained liver sections. Arrowheads indicate tumour nodules.

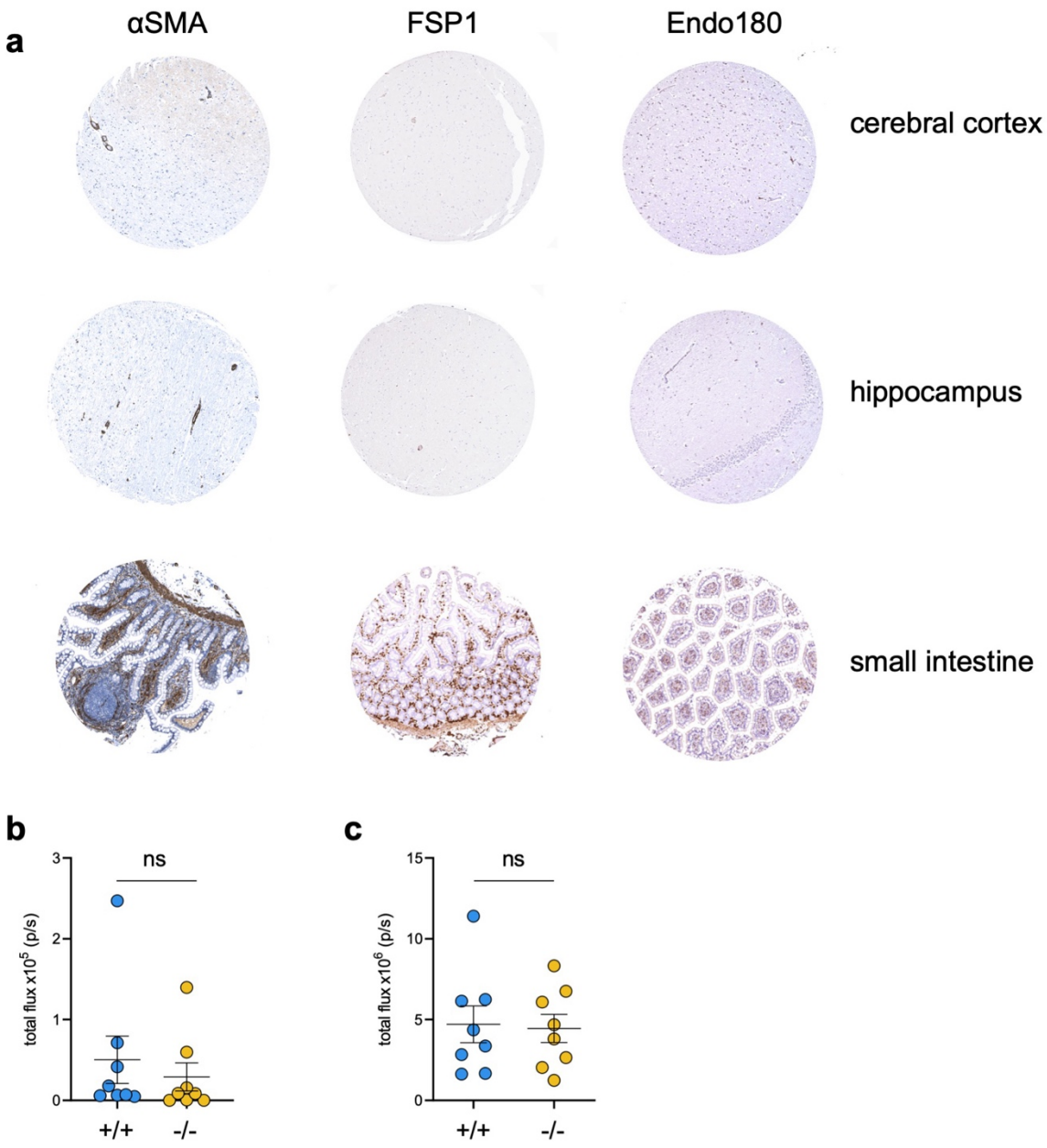

Supplementary Fig. 3 | Expression of Endo180 in the brain
a Images taken from The Human Protein Atlas of brain (cerebral cortex and hippocampus) and small intestine stained for Endo180 and the fibroblast markers αSMA and FSP1. **b** 2.5 x 10^3 4T1-Luc cells were injected intracranially (supraventorial) into BALB/c mice (n = 8 per group). Metastatic colonisation was measured by *ex vivo* IVIS imaging on day 12 (mean values ±SEM, *t*-test, no significant differences). **c** 3 x 10^5 4T1-Luc cells were injected into the left ventricle of the heart (n = 8 per group) and metastasis to the brain monitored by *in vivo* IVIS imaging on day 10 (mean values ±SEM, *t*-test, no significant differences). Related to Fig. 3.

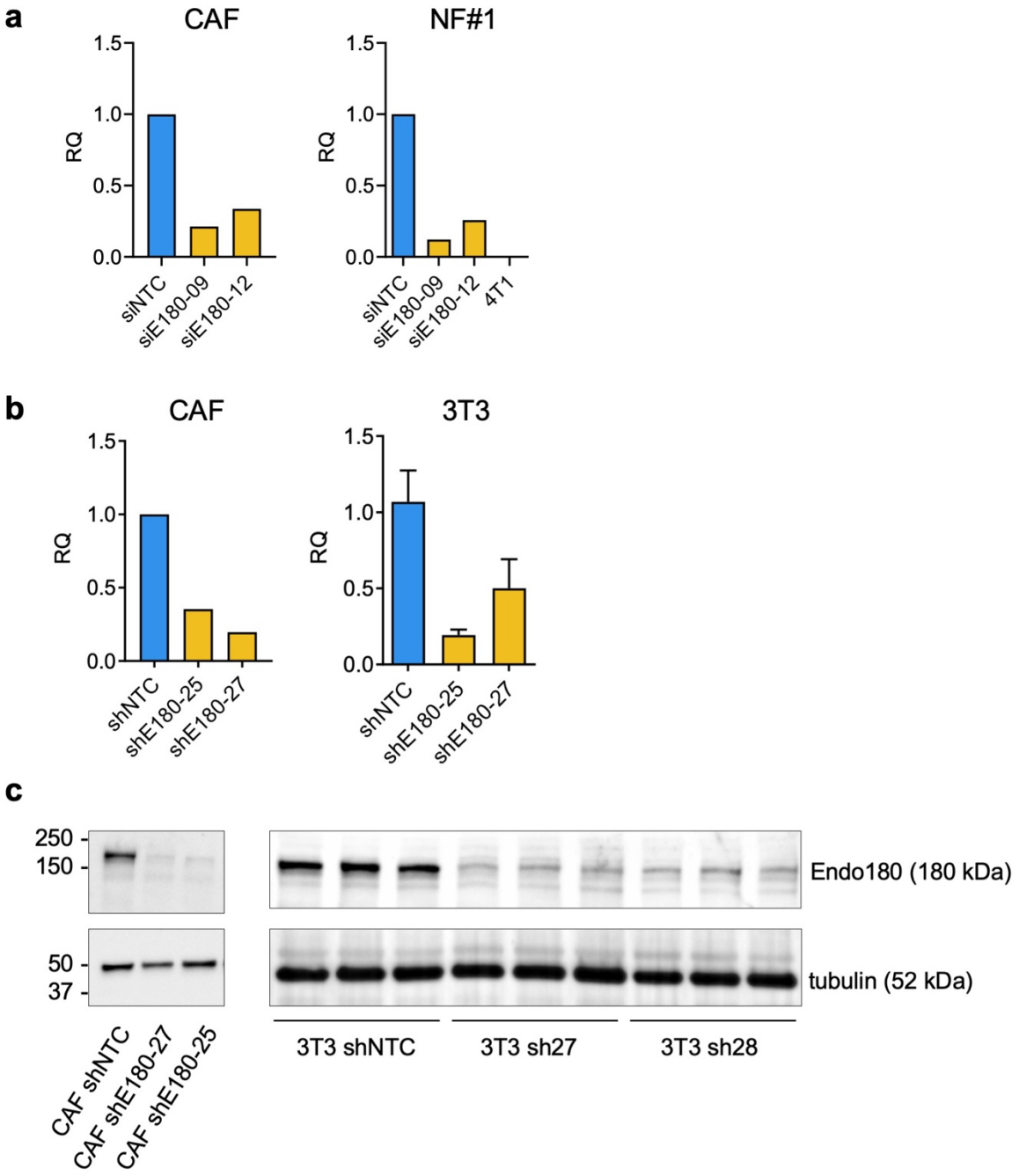

Supplementary Fig. 4 | Endo180 expression following siRNA- or shRNA-mediated knockdown

a, b Relative Endo180 (*Mrc2*) expression in CAFs and NF#1 and 3T3 mouse fibroblasts after transfection/ transduction with two independent (a) siRNAs or (b) shRNAs in comparison to non-targeting control (NTC) analysed by RT-qPCR. No expression was detected in 4T1 tumour cells. **c** Western blot of Endo180 (180 kDa) in CAFs (left panel) and 3T3 fibroblasts (right panel) transduced with either non-targeting control shRNA (shNTC) or two independent shRNAs against Endo180. Tubulin serves as loading control. Molecular size markers are in kDa. Related to Fig. 4.

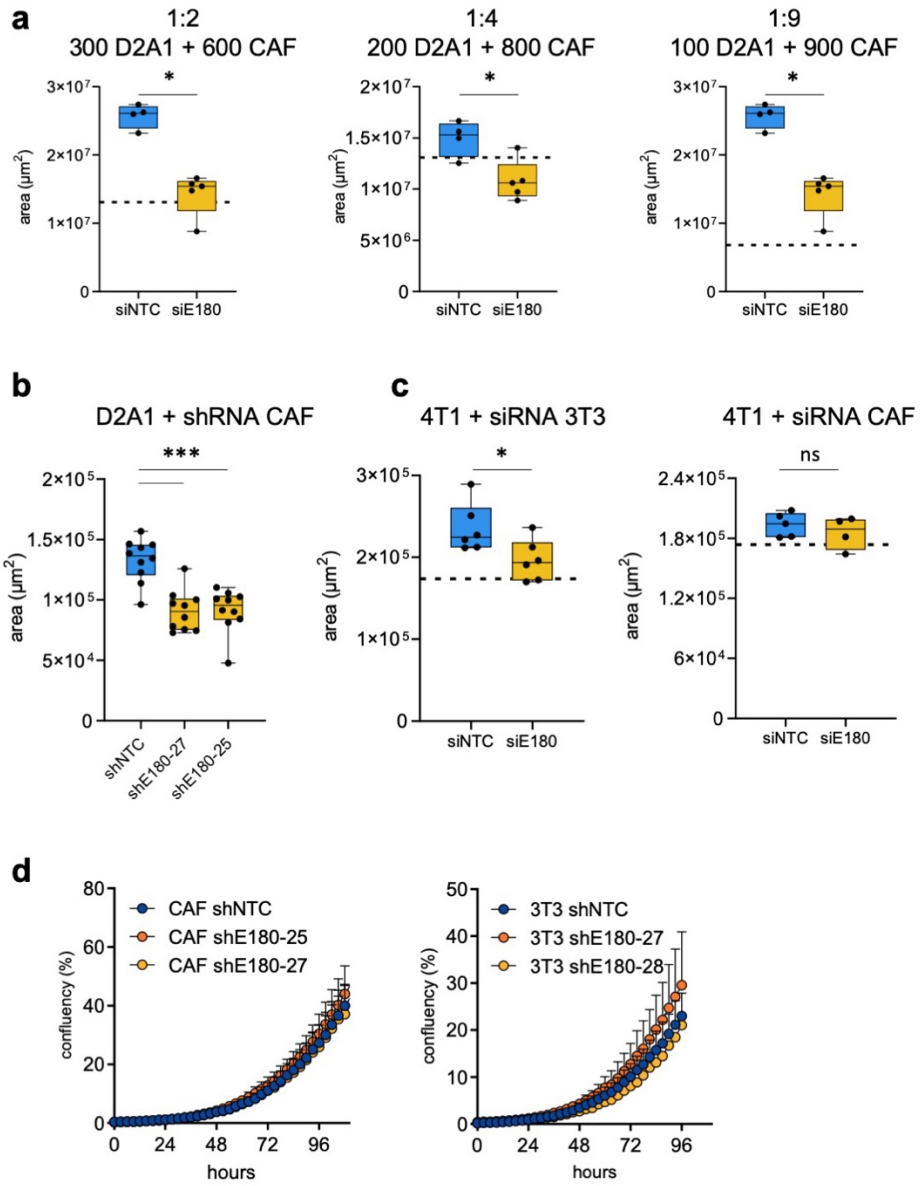

Supplementary Fig. 5 | Fibroblast-tumour cell co-culture assays
In all experiments, fibroblasts were transfected with non-targeting control or Endo180 si/shRNAs. **a** Different ratio of D2A1 and CAF cells were co-cultured in U-bottom low adherence plates (n = 4-5 spheroids per condition). Box plot shows median and 25th to 75th quartile, whiskers show minimum and maximum. Mean size of D2A1 spheroids alone is indicated by the dotted line (1:3 ratio, Mann-Whitney *U* test; 1:5 ratio *t*-test, 1:9 ratio Mann-Whitney *U* test). Related to Fig. 4a. **b** Equivalent results to panel a were obtained using CAFs transduced with shRNAs instead of siRNA. Shown are 1:3 ratio co-cultures of D2A1 and CAFs transduced with non-targeting (NTC) or two independent Endo180-targeting shRNAs after 6 days (n = 10 spheroids per condition; mean values ±SEM, one-way ANOVA). Related to Fig. 4a. **c** 4T1 cells admixed with 3T3 or CAFs in U-bottom low adherence plates and cultured for 8 days. Spheroid growth was assessed by spheroid area (n = 4-6 spheres per condition, mean values ±SEM, *t*-test). Related to Fig. 4b. **d** CAFs or 3T3 fibroblasts were cultured in 24-well plates in D2A1 conditioned medium prior to decelluarisation. D2A1 cells were plated onto the fibroblast-derived matrices and growth monitored by IncuCyte imaging (n = 3 wells per condition; mean values ±SEM, 2-way ANOVA). Related to Fig. 4g.

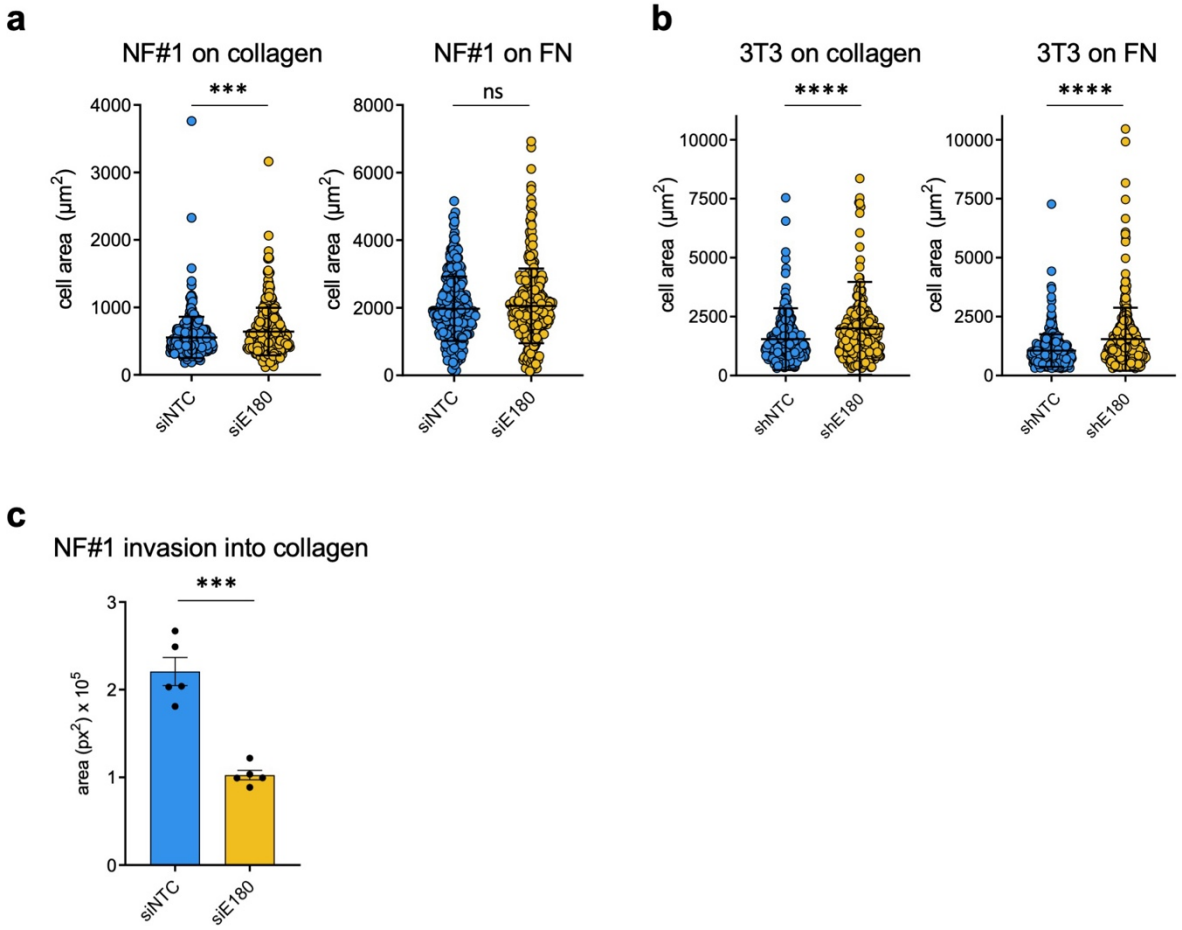

Supplementary Fig. 6 | Cell spreading on collagen or fibronectin-coated hydrogels
a,b Cell spreading (area) of siNTC and siEnd180 (siE180) NF#1 fibroblasts on collagen or fibronectin-coated hydrogels (50 kPa) and shNTC and shE180-27 3T3 fibroblasts on collagen or fibronectin-coated glass coverslips, respectively, (n = 300 cells; mean values ±SEM, Mann-Whitney *U* test). Related to Fig 5a,b. **c** Invasion of siNTC or siE180 NF#1 fibroblasts from 3D aggregates into a collagen matrix after 48 hours (n = 4; mean values ±SEM, *t*-test). Related to Fig. 5d.

Supplementary Figure 7

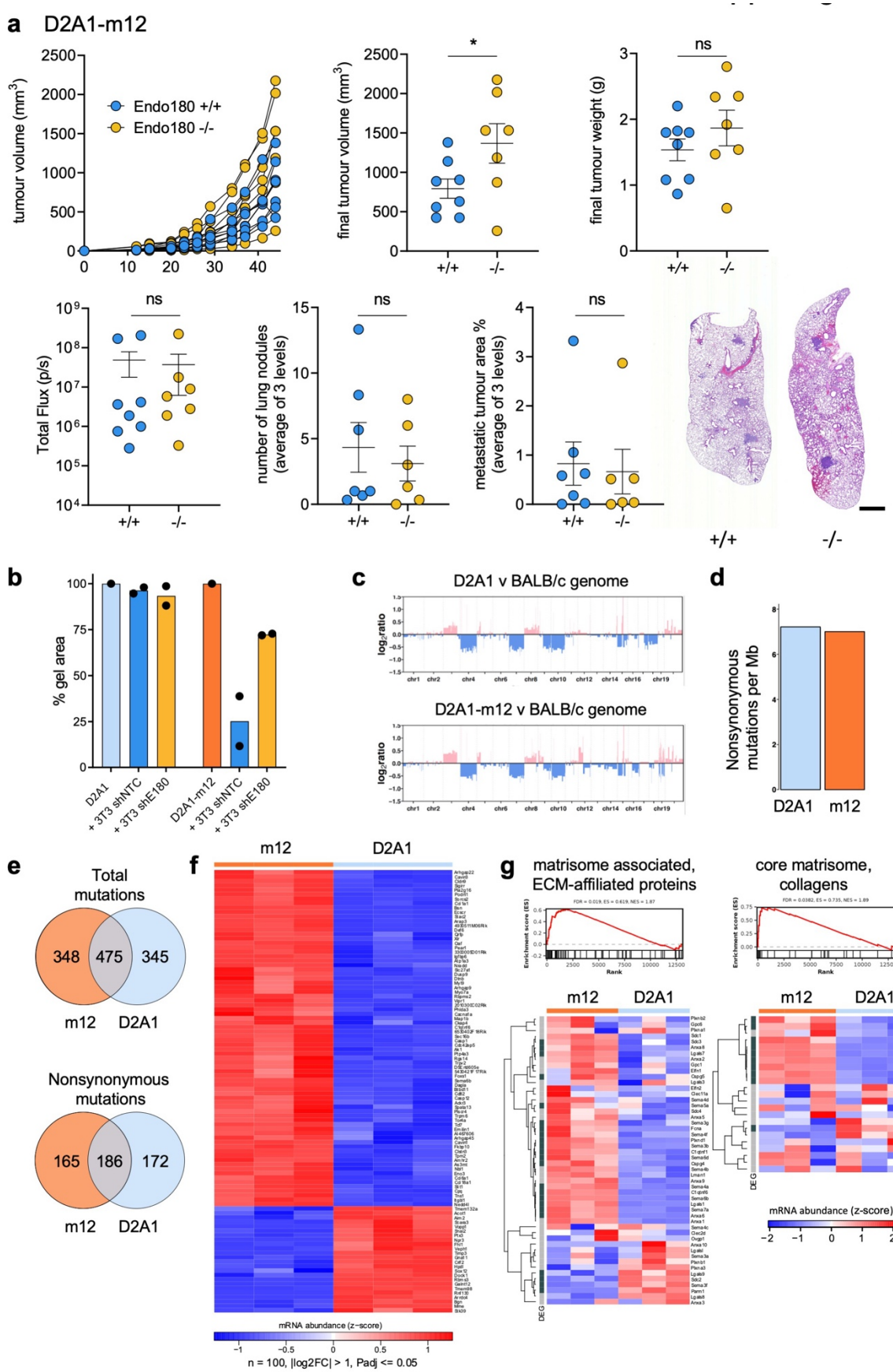

Supplementary Fig. 7 | Comparison of the parental D2A1 line and the D2A1-m12 subline

a 5 x 10^4 D2A1-m12-Luc cells were injected into the 4^{th} mammary fat pad of BALB/c Endo180$^{+/+}$ or Endo180$^{-/-}$ mice (n = 8 per group) and tumour volume measured twice weekly. The experiment was terminated on day 41. Shown are: D2A1-m12 primary tumour growth in individual mice, final tumour volume, primary tumour weights, quantification of metastatic burden by *ex vivo* IVIS imaging of the lungs, number of lung nodules and metastatic tumour area in the lungs. All data are mean values ±SEM (*t*-test). Representative H&E stained lung sections are shown (scale bar, 1 mm). Related to Fig. 7b. **b** shNTC or shEndo180 3T3 fibroblasts were embedded in a 1:1 ratio (each 5 x 10^5 mL^{-1}) with either D2A1 or D2A1-m12 tumour cells in collagen gels. Data show % gel contraction after 48 hours (n = 2). **c** Copy number variation plots (log_2 ratio) for D2A1 and D2A1-m12 cell lines using a reference BALB/c genome. **d** Tumour mutational burden of D2A1 and D2A1-m12 cell lines as determined using whole-exome sequencing (WES). **d** number of protein-coding nonsynonymous mutations per Mb of exome. **e** Venn diagrams illustrating the number of total mutations and nonsynonymous mutations in common between the D2A1 and D2A1-m12 cell lines. **f** Heatmap displaying mRNA abundance of top 100 significantly differentially expressed genes (DEGs) determined by RNA-seq, in D2A1-m12 compared with D2A1cells (n = 3; heatmap scale is a z-score). Threshold for differential expression was $|log_2FC| > 1$, and adjusted *P* value ≤ 0.05. **g** fGSEA of 'core matrisome, collagens' and 'matrisome-associated, ECM-affiliated proteins', and associated heatmaps showing the genes of the pathway (n = 3; heatmap scale is a z-score). Dark grey, significant DEGs with $|log_2FC| > 1$ and adjusted *P* value ≤ 0.05. Light grey, nonsignificant DEGs. Related to Fig. 7f.

References

1. Di Tommaso, P. *et al.* Nextflow enables reproducible computational workflows. *Nat Biotechnol* **35**, 316-319 (2017).
2. Li, H. & Durbin, R. Fast and accurate long-read alignment with Burrows-Wheeler transform. *Bioinformatics* **26**, 589-595 (2010).
3. Li, H. *et al.* The Sequence Alignment/Map format and SAMtools. *Bioinformatics* **25**, 2078-2079 (2009).
4. McKenna, A. *et al.* The Genome Analysis Toolkit: a MapReduce framework for analyzing next-generation DNA sequencing data. *Genome Res* **20**, 1297-1303 (2010).
5. Talevich, E., Shain, A.H., Botton, T. & Bastian, B.C. CNVkit: Genome-Wide Copy Number Detection and Visualization from Targeted DNA Sequencing. *PLoS Comput Biol* **12**, e1004873 (2016).
6. Wilm, A. *et al.* LoFreq: a sequence-quality aware, ultra-sensitive variant caller for uncovering cell-population heterogeneity from high-throughput sequencing datasets. *Nucleic Acids Res* **40**, 11189-11201 (2012).
7. Wang, K., Li, M. & Hakonarson, H. ANNOVAR: functional annotation of genetic variants from high-throughput sequencing data. *Nucleic Acids Res* **38**, e164 (2010).
8. Wienke, D. *et al.* The collagen receptor Endo180 (CD280) Is expressed on basal-like breast tumor cells and promotes tumor growth in vivo. *Cancer Research* **67**, 10230-10240 (2007).
9. Calon, A. *et al.* Dependency of colorectal cancer on a TGF-beta-driven program in stromal cells for metastasis initiation. *Cancer cell* **22**, 571-584 (2012).